SEMARAK ILMU PUBLISHING

Journal of Advanced Research in Applied Sciences and Engineering Technology

Journal homepage:
https://semarakilmu.com.my/journals/index.php/applied_sciences_eng_tech/index
ISSN: 2462-1943

Optimized bi-Quadratic Trigonometric Bézier Curve using Particle Swarm Optimization

Mohamad Ekram Nordin[1], Md Yushalify Misro[1,*]

[1] School of Mathematical Sciences, Universiti Sains Malaysia, 11800, Gelugor, Pulau Pinang, Malaysia

ARTICLE INFO

Article history:
Received 2 July 2023
Received in revised form 13 September 2023
Accepted 2 November 2023
Available online 19 November 2023

Keywords:
biarcs; optimized biarc; particle swarm optimization; quadratic; trigonometric Bézier

ABSTRACT

This paper introduces a new approach, namely an optimized bi-QT-Bézier, for fitting curves to given 2D polygons and their two end tangents. The conventional approach includes additional constraints to uniquely determine the biarc. The main idea is to exploit the inherent freedom in the choice of the α to achieve an optimized curve that is closer to its control polygon. The proposed method integrates the formulation of a single biarc with the Quadratic Trigonometric (QT)-Bézier curve and Particle Swarm Optimization (PSO). The proposed bi-QT-Bézier is advantageous in curve fitting as it provides an optimized value of α from the PSO method. Besides, the proposed scheme also provides the flexibility to construct the desired curve. The proposed approach generates a curve with a smaller distance between the curve and its control polygon compared to the previous optimal single biarc and Sabin's constraint. An experimental result is provided to demonstrate the usefulness and efficiency of the proposed method. The implementation of the optimized bi-QT-Bézier to fit a circle and complex shape will also be analyzed. This proves that the proposed method is an excellent tool in curve fitting.

1. Introduction

A biarc is widely used for arc spline approximation [1–9]. A biarc consists of two smoothly connected circular arcs that interpolate two endpoints and two end tangents [1–6]. According to Bolton [5], the biarc is used to replace the conventional approach of curve fitting, which is a cubic spline. For the biarc to be C^1 or G^1 continuous, the two arcs must have the same tangent at the intersection point. The conventional biarc fitting comprises additional constraints to determine the biarc uniquely. For example, Bolton proposed a constraint with equal angles of the two arcs to minimize the difference in the radii of the circular arcs. The work by Bolton also provided new insight into the potential application of biarcs and inspired scholars to study the biarc extensively.

Furthermore, Meek and Walton [6] and Schönherr [7] proposed a biarc, where the intersection point lies on the bisector of the line segment connecting the two endpoints. As a result, the difference in the curvatures of the two arcs can be minimized. The study by Meek and Walton [6] also reports

* *Corresponding author.*
E-mail address: yushalify@usm.my

https://doi.org/10.37934/araset.33.3.258278

that the longest arc method could approximate to a certain accuracy with fewer biarcs than the bisection method. The bisection method finds the approximation quickly but uses more biarc than the longest arc method. Moreover, Sabin in [8] proposed a biarc with an additional constraint, where the tangent at the joining point is parallel to the line connecting the two endpoints. The study reported that the ratio of the two radii can be as close to 1, which indicates the robustness of the biarc [1–4].

However, these claims can be contended by the study by Park [1, 2] and Ong *et al.,* [9], who have not imposed any additional constraints on the proposed biarcs. The study by Ong *et al.,* [9] proposed a formulation of the curve fitting problem to achieve a better fit. The study reported that the total area between the biarc spline and B-spline curves could be minimized which indicates a better approximation. Besides, the studies by Park [1, 2] proposed an optimal single biarc that exploits the choices of biarc. The studies reported that the proposed approach minimized the distance between the biarc and polygon. The studies also reported that proposed approach manage to reduce the number of segments in the resulting arc spline.

An optimization algorithm is a method or procedure used to find the best solution or set of solutions to a problem that maximizes or minimizes a particular objective function. Many optimization algorithms are frequently used to find optimal parameters in curve and surface optimization, and curve fitting. The studies by Gulsen e*t al.,* [10] and Kumar *et al.,* [11] proposed Genetic Algorithm (GA) in curve fitting. According to Gulsen *et al.,* [10], the GA was reasonably robust in finding the optimal values of parameters that minimizes the total error on a set of data points. However, Kumar *et al.,* [11] reported that GA has a higher-cost solution where the convergence slows down when the generations proceed and get closer to the optimal solution.

The optimization algorithm such as PSO is flexible and can be used in various fields. The study by Ng *et al.,* [12] applied the PSO in the context of biology. On the other hand, the study by Gálvez and Iglesias [13] proposed a Particle Swarm Optimization (PSO) algorithm in curve fitting to compute an optimal location of knots. According to Gálvez and Iglesias, the PSO is more accurate even for curves with singularities or cusps. In addition, BiBi *et al.,* [14] and Liu and Li [15] utilized the PSO algorithm to find the optimum values of shape parameters. BiBi *et al.,* [14] reported that the PSO increases the desired parameters' optimality to achieve a high developability degree of developable surface. The study by Liu and Li [15] shows that the parameters obtained by PSO make the smoothness of the curve with solid portability which implies that PSO manage to find an optimal parameter.

The study by Eshan *et al.,* [16] investigates the effect of the shape parameter on the equation formed via the Moving Least Square (MLS) Method. The study reported that the shape parameter plays a large factor in the curve fitting. Additionally, Adnan *et al.,* [17] use multiple degrees of trigonometric Bézier curves to fit more complex shapes, whereas continuous trigonometric Bézier curves can be used to construct a smooth surface [18]. Uzma *et al.,* [19], Han [20], and Wu *et al.,* [21] report that the Quadratic Trigonometric (QT)-Bézier curve manages to pull the curve closer to the control polygon. The studies provide a detailed definition and properties of the QT-Bézier basis function. Moreover, according to Misro *et al.,* [22, 23], trigonometric Bézier with shape parameters could provide flexibility in constructing the curve. This statement is supported by Xu *et al.,* [24] that discussed the adjustable quadratic trigonometric polynomial Bézier curves with a shape parameter.

Therefore, this paper introduced an optimized bi-QT-Bézier that utilizes the freedom of α. The bi-QT-Bézier is a curve formed by connecting two QT-Bézier curves in a G^1 continuity manner. It should be noted that α and β are the lengths of the two sides of the isosceles control triangle of the first curve and the second curve, respectively. Apart from that, this paper aims to achieve an optimized curve that is closer to its control polygon. Even though the previous study by Park [1,2] and Ong *et al.,* [9] do not imposed any additional constraint in their proposed biarcs, but they also

do not utilize any optimization algorithm. Thus, this study incorporates the optimal single biarc using the Quadratic Trigonometric (QT) Bézier curve with an optimization method, namely the PSO algorithm. In this paper, the optimized bi-QT-Bézier is applied in the curve fitting of a given 2D polygon with its two-end tangents to produce an optimal curve fitting. The implementation of the optimized bi-QT-Bézier to fit a circle and a complex shape will also be analyzed.

The work is organized as follows. In Section 2, the concept of the QT-Bézier curve, as well as the optimal single biarc, is presented. The formulation of the PSO method, the length of the arc, the curvature formulation and the percentage error are also provided. Subsequently, in Section 3, the proposed method is implemented to fit two different shapes, and the effectiveness of the proposed method is discussed. Finally, the conclusion and the recommendation for future works are addressed in Section 4.

2. Methodology

2.1 Quadratic Trigonometric Bézier Curve

The Quadratic Trigonometric (QT) Bézier basis function with a shape parameter can minimize the distance between the curve and the control polygon. For $u \in [0, 1]$, the QT basis function with shape parameter m for $m \in [-1, 1]$ are defined as in Equation (1) by Uzma *et al.,* [19].

$$\begin{cases} f_0(u) = \left(1 - \sin\frac{\pi}{2}u\right)\left(1 - m\sin\frac{\pi}{2}u\right), \\ f_1(u) = (1+m)\left(\cos\frac{\pi}{2}u + \sin\frac{\pi}{2}u - 1\right), \\ f_2(u) = \left(1 - \cos\frac{\pi}{2}u\right)\left(1 - m\cos\frac{\pi}{2}u\right). \end{cases} \quad (1)$$

The QT basis function defined in Equation (1) has the following properties according to Uzma *et al.,* [19]:

a. Non-negativity: $f_i(u) \geq 0, i = 0, 1, 2.$
b. Partition of unity: $\sum_{i=0}^{2} f_i(u) = 1.$
c. Monotonicity: As shown in Figure 1, f_0 (black) is monotonically decreasing, and f_2 (pink) is monotonically increasing for a given value of the parameter m.
d. Symmetry:$f_i(u; m) = f_{2-i}(1 - u; m)$, for $i = 0, 1, 2.$

Figure 1 shows the QT-Bézier basis function for $m = -1$ and $m = 1$; $f_0(u)$ (black); $f_1(u)$ (red); $f_2(u)$ (pink). Given the control points, p_i $(i = 0, 1, 2)$, the QT-Bézier with single shape parameter is defined as Equation (2).

$$f(u) = \sum_{i=0}^{2} f_i(u)p_i. \quad (2)$$

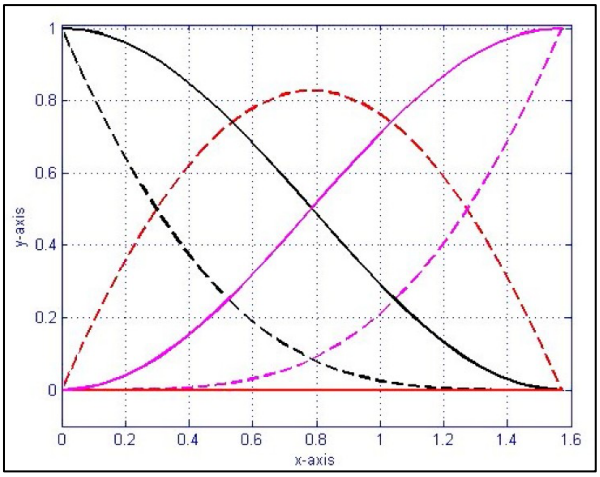

Fig. 1. The QT-Bézier basis function for m = 1 (dashed) and for m = –1 (solid)

Note that, when the shape parameter $m = 0$, the QT-Bézier will behave as a classical quadratic Bézier curve. The QT-Bézier has the following properties:

a. Endpoint properties:
$f(0) = p_0, \ f(1) = p_2$

$f'^{(0)} = (1+m)(p_1 - p_0), \ f'(1) = (1+m)(p_2 - p_1)$

$f''(0) = 2mp_0 - (1+m)p_1 + (1-m)p_2, \ f''(1) = 2mp_2 - (1+m)p_1 + (1-m)p_0$

$f'''(0) = -(1+m)(p_1 - p_0), \ f'''(1) = -(1+m)(p_2 - p_1)$

Remark
(i) $f^{2k+1}(0) = (-1)^k f'(0)$ and $f^{2k+1}(1) = (-1)^k f'(1), \quad k = 1, 2, 3, \dots, n$
(ii) Inverting the order of the control points, all derivatives of order $2k, \ k = 1, 2, 3, \dots, n$ coincide.

b. Symmetry: $p_0, \ p_1, \ p_2$ and $p_2, \ p_1, \ p_0$ define the same curve in different parametrizations.
c. Geometric invariance: The shape of the curve created is independent of the choice of coordinates.
d. Convex hull property: From the non-negativity and partition of unity of basis function, the whole curve is located in the convex hull generated by its control points.

2.2 Optimal Single Biarc

Given two endpoints, p_0 and p_4, with their respective end tangents, t_1 and t_2, a biarc consists of two circular arcs with G^1 continuity as a joining point and can be defined with five control points p_i where $i = 0, 1, 2, 3, 4$. As shown in Figure 2, the two arcs have the same tangent (red solid tangent) at the intersection point. It implies that the tangent has the same direction at the intersection point. To achieved G^1 continuity, the intersection point, p_2 must be collinear with its neighbour control points, which are $p_1$and p_3. In addition, the ratio of lengths $\alpha = ||p_1p_2||$ and $\beta = ||p_2p_3||$ are not fixed as the value α and β not necessarily equal to each other unless the ratio, $r = 1$.

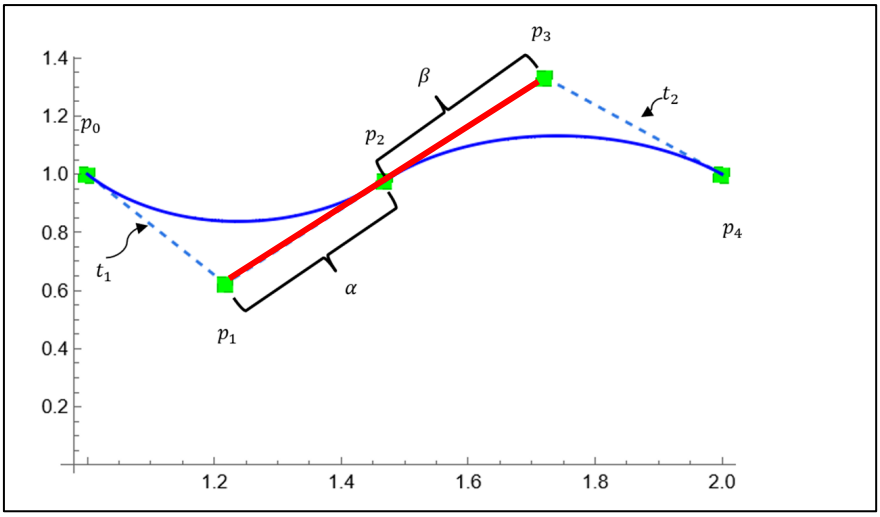

Fig. 2. Biarc formulation

By adopting the optimal single biarc method proposed by Park [1, 2], the ratio r that generates a biarc with a small distance between the curve and control polygon can be obtained. As described in [1-4], the value of α can be obtained by solving Equation (3)

$$v.v + 2\alpha v.(rt_1 + t_2) + 2r\alpha^2(t_1t_2 - 1) = 0, \tag{3}$$

where the distance between endpoints, $v = p_4 - p_0$, the ratio, $r = \frac{\alpha}{\beta}$, with the end tangent vectors are defined as follows; $t_1 = (\cos\theta\,, \sin\theta)$ and $t_2 = (\sin\theta\,, -\cos\theta)$. The value of α and β are always positive as discussed by Piegl *et al.*, [3, 4]. The control points, p_1, p_2 and p_3, are determined using Equation (4), Equation (5), and Equation (6), respectively.

$$p_1 = p_0 + \alpha t_1, \tag{4}$$

$$p_2 = \frac{\beta}{\alpha + \beta}p_1 + \frac{\alpha}{\alpha + \beta}p_3, \tag{5}$$

$$p_3 = p_4 - \beta t_2. \tag{6}$$

The integer value of d, a real number of ρ, where 0 < ρ < 1, the upper limit (r_u), center (r_c) and lower limit (r_l), are initialized. Consequently, the range of the ratios is computed using Equation (7) and Equation (8). The ratio values of, r_i and r_{d+i} are determined by Equation (9) and Equation (10).

$$\Delta R_l = \begin{cases} \frac{1}{r_l} - \frac{1}{r_c}, & 0 < r_l < r_c \leq 1, \\ r_c - r_l, & 1 \leq r_l < r_c, \end{cases} \tag{7}$$

$$\Delta R_r = \begin{cases} \frac{1}{r_c} - \frac{1}{r_u}, & 0 < r_c < r_u \leq 1, \\ r_u - r_c, & 1 \leq r_c < r_u, \end{cases} \tag{8}$$

$$r_i = \begin{cases} \left(\left(\frac{d-i}{d}\right)\frac{1}{r_l} + \left(\frac{i}{d}\right)\frac{1}{r_c}\right)^{-1}, & 0 < r_l < r_c \leq 1, \\ \left(\frac{d-i}{d}\right) r_l + \left(\frac{i}{d}\right) r_c, & 1 \leq r_l < r_c, \end{cases} \tag{9}$$

$$r_{d+i} = \begin{cases} \left(\left(\frac{d-i}{d}\right)\frac{1}{r_c} + \left(\frac{i}{d}\right)\frac{1}{r_u}\right)^{-1}, & 0 < r_c < r_u \leq 1, \\ \left(\frac{d-i}{d}\right) r_c + \left(\frac{i}{d}\right) r_u, & 1 \leq r_c < r_u. \end{cases} \tag{10}$$

For each ratio, the distance between the biarc, $\boldsymbol{B}$ and control polygon, $\boldsymbol{P}$ is computed using Equation (11) and Equation (12).

$$dist(\boldsymbol{P}, \boldsymbol{B}) = max_{i=0}^{n}\, dist\big(p_i, A_{j(i)}\big), \tag{11}$$

$$dist\big(p_i, A_{j(i)}\big) = \big||p_i - p|\big| = rad_{j(i)} - ||p_i - c_{j(i)}||, \tag{12}$$

where p_i is the points on control polygon, $A_{j(i)}$ denotes the points on the arc. Meanwhile in Equation (12), $rad_{j(i)}$ is the radius of the arc and $c_{j(i)}$ is its center.

Index j that leads to a biarc with the minimum value is determined and the tolerance value is set to be $r = 10^{-4}$. Next, by replacing the domain with a smaller one in the vicinity, $r_l \leftarrow r_{j-1}, r_c \leftarrow r_j,\ r_u \leftarrow r_{j+1}$, the value of d_{new} is updated as in Equation (13). Finally, the process will be repeated until the optimal ratio is obtained.

$$d_{new} = \max(2, int(1-\rho)\, d). \tag{13}$$

2.3 Particle Swarm Optimization

The value of α plays a vital role in generating the biarc. However, the optimized bi-QT-Bézier does not obtain the value of α by solving Equation (3). Instead, the optimized bi-QT-Bézier finds the optimal value of α using the optimization method. The optimal value of the α obtained from the optimization method is denoted as $\bar{\alpha}$. It is worth mentioning that the $\bar{\alpha}$ converges in a bounded range of real numbers. Therefore, Theorem 1 is proposed to indicate that the mentioned range are always converges.

Theorem 1. *The value of the optimized $\bar{\alpha}$ is always converges between $[\alpha - \varepsilon,\ \alpha]$.*
Proof. Let $\alpha \in \mathbb{R}$ and let $\varepsilon > 0$, the ε-neighbourhood of α is denoted $V_{\in(\alpha)} := \{x \in \mathbb{R}: \alpha - \varepsilon < x < \alpha + \varepsilon\}$. Since the terms in $V_{\in(\alpha)}$ are in order and increasing, therefore $V_{\in(\alpha)}$ is a monotone sequence. By Monotone Convergence Theorem, a monotone sequence converges if and only if it is bounded. Hence, $V_{\in(\alpha)}$ is converges. By Bolzano Weierstrass Theorem, every bounded sequence of real numbers has a convergent subsequence. Thus, the subsequence of $V_{\in(\alpha)}$, $[\alpha - \varepsilon,\ \alpha]$ also converges.

After the ratio is obtained, the specified solution space, $[Z_{min}, Z_{max}]$, and the parameters of the problem, which are the number of dimensions (D), the lower bound (χ_1) and the upper bound (χ_2), are initialized. Correspondingly, the parameters of the algorithm, which are the number of particles (N), number of iterations ($Iter$), cognitive coefficient (c_1), social coefficient (c_2), random variables

r_1 and r_2, and weight inertia (ω), are set. Variables r_1 and r_2 are random between 0 and 1. A fitness function $R(x)$ that gives the optimal value of α is defined in Equation (14).

$$R(x) = v.v + 2xv.(rt_1 + t_2) + 2rx^2(t_1t_2 - 1). \quad (14)$$

After the movement of each particle is updated, the p_{best} and g_{best} can be determined using Equation (15) and Equation (16), respectively.

$$p_{best} = \begin{cases} x_i, & if\ R(x_i) > R(p_{best}), \\ p_{best}, & otherwise, \end{cases} \quad (15)$$

$$g_{best} = \begin{cases} x_i, & if\ R(x_i) > R(g_{best}), \\ g_{best}, & otherwise. \end{cases} \quad (16)$$

The new particles' velocity and position are updated using Equation (17) and Equation (18), respectively. If the termination criterion defined in Equation (19) does not meet, the algorithm will be repeated with the new updated velocity and position of particles. Otherwise, the optimal value of $\bar{\alpha}$ is obtained.

$$v_{ij}(k+1) = \omega.v_{ij}(k) + c_1r_1\left(p_{best_{ij}} - x_{ij}(k)\right) + c_2r_2\left(g_{best_{ij}} - x_{ij}(k)\right), \quad (17)$$

$$x_{ij}(k+1) = x_{ij}(k) + v_{ij}(k), \quad (18)$$

$$Z_{min} \leq g_{best} \leq Z_{max}. \quad (19)$$

After obtaining the new value of optimal $\bar{\alpha}$, the new control points can be determined. Note that an optimized bi-QT- Bézier can be generated with a minimum distance between the curve and the control polygon. The mechanism of optimized bi-QT-Bézier is described in Figure 3.

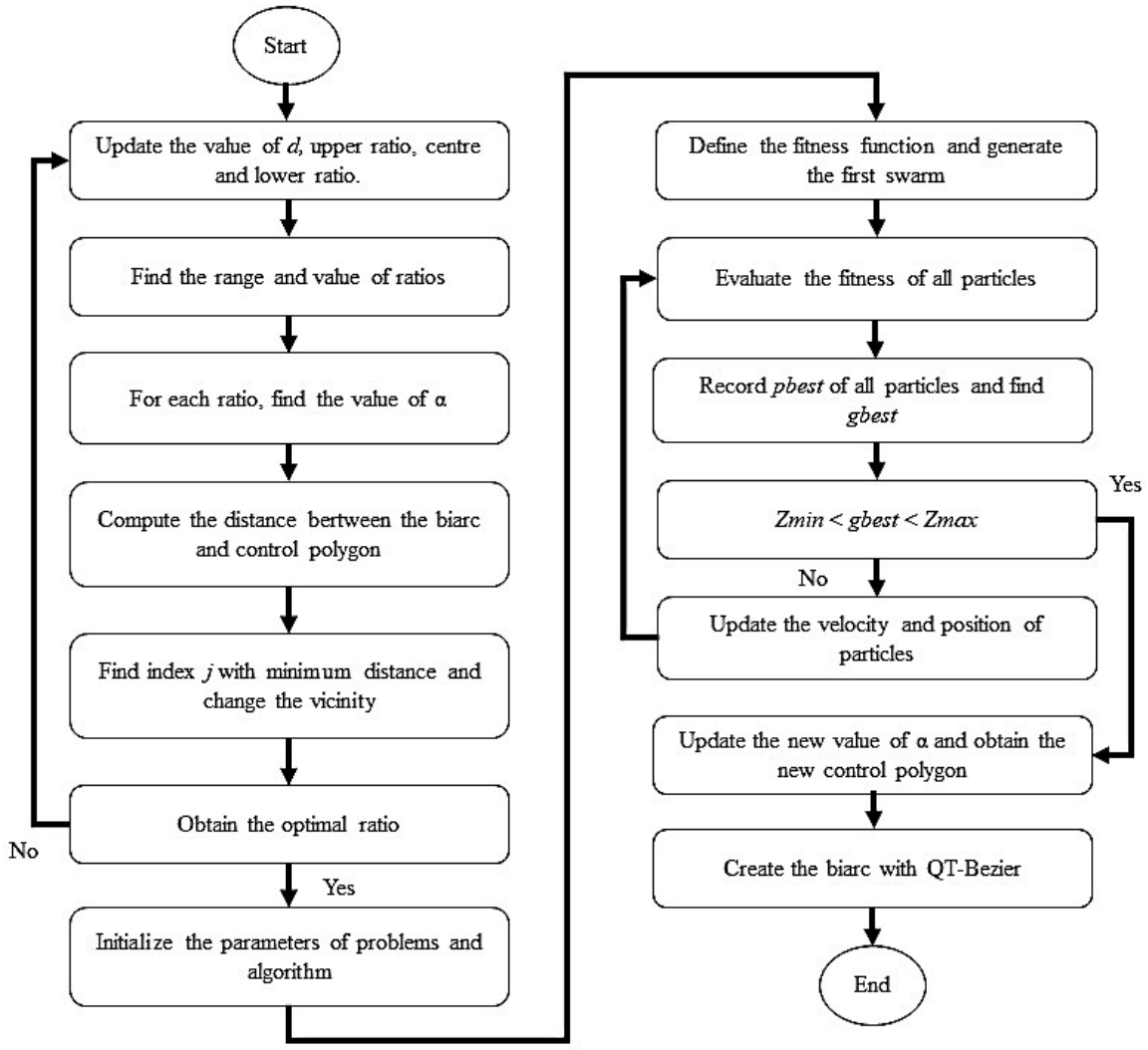

Fig. 3. Flowchart of the Optimized bi-QT-Bézier

2.4 Length of Arc

Assume that the given data points $p_i = (x_i, y_i), i = 1, 2, 3, \dots, N$, are distinct where the points are used to generate the approximate curve. The accuracy of the curve fitting is higher if the total length of the curves is approaching and closer to the shape's perimeter. Hence, the length of arc, L_A, used in approximating the shape is defined as Equation (20).

$$L_A = \int_0^1 \sqrt{\left(\frac{dx}{du}\right)^2 + \left(\frac{dy}{du}\right)^2}\, du. \tag{20}$$

2.5 Curvature Formulation

Let $z(t) = (x(t), y(t))$ be a parametric representation. The curvature formulation, κ is defined as Equation (21).

$$\kappa = \frac{x'y'' - y'x''}{(x'^2 + y'^2)^{3/2}}. \tag{21}$$

where primes refer to derivatives with respect to t.

2.6 Percentage Error

Percentage error shows the magnitude of the approximation errors throughout an analytical procedure. Likewise, the percentage error of the curve fitting for both approaches, optimized bi-QT-Bézier and optimal single biarc, is calculated. The curve fitting approach has a good approximation when the percentage error is closer to 0. The percentage error can be calculated using Equation (22).

$$Error = \frac{|Approximate - Exact|}{Exact} \times 100. \tag{22}$$

3. Results and Discussion

3.1 Enclosed in Rectangle

The proposed approach is applied to an example enclosed in a 3.6×5.9 rectangle where the two endpoints and two end tangents are given as $p_0 = (0, 3.6), p_4 = (5.9, 0), t_1 = (\cos 0\,,\ \sin 0),\ t_2 = (\sin 10\,,\ -\cos 10)$. Note that the values d, r_u, r_c, r_l and ρ are arbitrarily chosen. In this example, the value of $d,\ r_u,\ r_c,\ r_l$ and ρ are initialized as 10, 5, 1, 0.2, and 0.25, respectively. The values are taken based on an example that are discussed in Park [1].

The ratio, r, is obtained to be 0.6765 using the optimal single biarc as proposed by Park [1,2]. Subsequently, the value of optimized $\bar{\alpha}$ can be found utilizing Particle Swarm Optimization (PSO). Table 1 shows the parameters of the problem and algorithm. The PSO was run three times until the optimal $\bar{\alpha}$ was obtained. Table 2 presents the value of $\bar{\alpha}$ for every iteration obtained for each simulation.

Table 1
List of Parameters

Problem Parameters		Algorithm Parameters	
Lower Limit (Z_{min})	2.2605	Number of Particle (N)	50
Upper Limit (Z_{max})	2.4105	Iterations (*iter*)	1000
Dimension (D)	1	Cognitive Coefficient (c_1)	2
Lower Bound (χ_1)	1	Social Coefficient (c_2)	2
Upper Bound (χ_2)	2	Weight Inertia (ω)	0.9

Based on Table 2, each simulation of the proposed method gives a different value of $\bar{\alpha}$. For example, in Simulation 1, the value of $\bar{\alpha}$ obtained is 2.36239, which is lower compared to the value of α obtained from solving Equation (3), which is 2.4105. Similarly, the $\bar{\alpha}$ obtained in Simulations 2 and 3 are 2.29967 and 2.35683, which are also lower than 2.4105. In addition, Simulations 1, 2, and 3 undergo 23, 30, and 44 iterations on the fitness function defined in Equation (14). This demonstrates that the PSO approach is an iterative optimization process that repeats the iterations until the stopping criterion is met.

Table 2
Value of optimal $\bar{\alpha}$ obtained from 3 simulations

No of iteration	Simulation 1	Simulation 2	Simulation 3
1	13.35770	3.16837	1.89576
2	2.02842	5.89204	6.85565
3	3.66474	11.65050	14.11530
4	4.87801	2.86155	3.13421
5	2.54995	12.35160	4.74028
6	2.53688	1.72255	9.42821
7	4.95763	4.30267	21.98950
8	2.47567	1.42392	3.87729
9	19.46630	5.85734	1.96328
10	2.98065	6.46450	3.86433
11	4.93813	5.03616	2.47194
12	1.88883	4.73585	10.27230
13	2.45019	3.33900	21.21920
14	2.08085	25.43440	2.70133
15	19.99810	13.06210	5.82390
16	1.74749	8.21273	3.49449
17	2.02265	3.47778	13.22040
18	3.63698	8.27582	4.16537
19	3.26113	6.24671	8.11610
20	4.40774	3.14243	2.48032
21	4.04289	3.86054	5.76370
22	10.40250	2.96846	2.55952
23	2.36239	8.74674	8.81185
24		2.17477	11.97070
25		3.34919	4.49595
26		10.78820	2.26041
27		8.03378	19.84340
28		3.34361	4.33171
29		8.28579	11.60080
30		2.29967	1.96053
31			5.58939
32			5.12272
33			3.95935
34			4.39231
35			7.03961
36			1.77828
37			1.83487
38			1.79398
39			4.00536
40			6.95418
41			3.71167
42			6.95975
43			3.12601
44			2.35683

Figure 4 illustrates the trends of the PSO algorithm in finding the optimal value of $\bar{\alpha}$. Based on Figure 4, the first 15 iterations of each graph fluctuate higher compared to the rest of the graph. This indicates that the particle velocities build up faster in the first 15 iterations. In this phase, the particles can move freely in the search space and eventually decrease over time. Note that the particle velocity is crucial in the PSO algorithm as it is considered the step size of the swarm by Engelbrecht and Andries [25]. At each step, the particles adjust the velocity and move in every direction of the search space. Hence, the process is shifting from the exploratory mode to the exploitative mode.

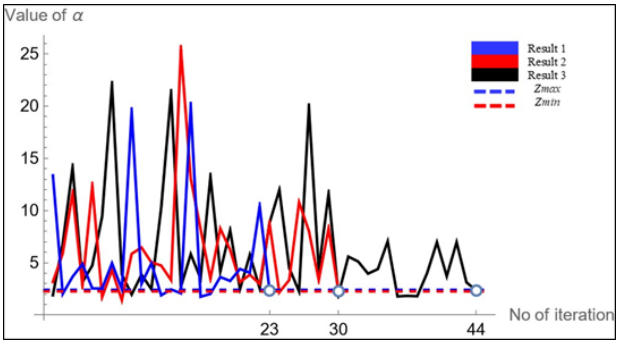

Fig. 4. Trends of the Particle Swarm Optimization

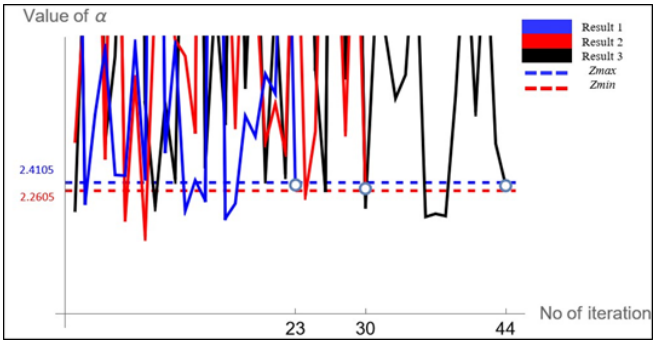

Fig. 5. Closed up of Figure 4

Consequently, Figure 5 displays that the optimal $\bar{\alpha}$ values obtained from each simulation are between Z_{min} and Z_{max}. The graph shows that the optimization algorithm converges to a specific value inside the solution space. Moreover, the number of iterations needed for each simulation to obtain an optimal value of $\bar{\alpha}$ varies. All simulations obtained the value of $\bar{\alpha}$ in less than 50 iterations. Thus, it shows that the proposed optimization algorithm is computationally efficient.

Table 3 compares the distance between the curve and control polygon for different values of α. Based on Table 3, the value of α obtained using the optimal single biarc is 2.4105, which gives a greater distance between the curve and the control polygon compared to the optimal $\bar{\alpha}$ obtained by the PSO algorithm. Hence, it demonstrates that the proposed method improved the curve fitting compared to the optimal single biarc. Furthermore, among the values of $\bar{\alpha}$ obtained by the proposed method, Simulation 2 has the smallest distance between the curve and control polygon, with $\bar{\alpha} = 2.299670$. The smaller the distance between the curve and the control polygon, the curve fitting will become better. Therefore, it can be concluded that the closer the value of $\bar{\alpha}$ to Z_{min}, the higher the optimality of the $\bar{\alpha}$. Therefore, the value of $\bar{\alpha}$ obtained from Simulation 2 is chosen as the optimal $\bar{\alpha}$.

Table 3
Distance between curve and control polygon obtained from different α or $\bar{\alpha}$

Approach	α or $\bar{\alpha}$	Distance
Optimal Single Biarc	2.410500	0.377760
PSO Simulation 1	2.362390	0.376162
PSO Simulation 2	2.299670	0.375021
PSO Simulation 3	2.356830	0.376017

Note that the value of the shape parameter, m, is set to be 0, which imitates the behavior of the standard Bézier curve, to compare the proposed approach with the previous work by Park [1,2] and Sabin [8]. Figures 6a, 6b, and 6c reveal the curve generated with α obtained using Sabin's constraint, optimal single biarc, and optimized bi-QT-Bézier, respectively. Curves generated by optimized $\bar{\alpha}$ has the smallest distance compared to the biarcs generated by Sabin's constraint and optimal single biarc. Therefore, the curves created with $\bar{\alpha}$ obtained using the proposed method outperforms the optimal single biarc by Park [1,2] and by Sabin's constraint [8]. Table 4 shows the distance between the curve and the control polygon obtained from different values of the shape parameter, m.

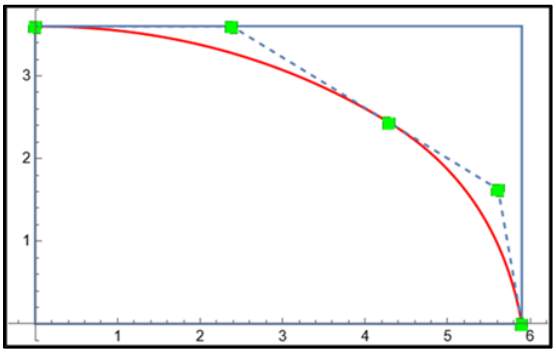

(a) Sabin's constraint ($r = 0.6943, \alpha = 2.38084, distance = 0.387271$)

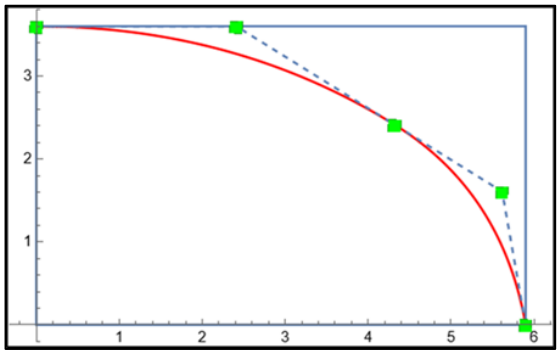

(b) Optimal Single Biarc ($r = 0.6765, \alpha = 2.4105, distance = 0.377760$)

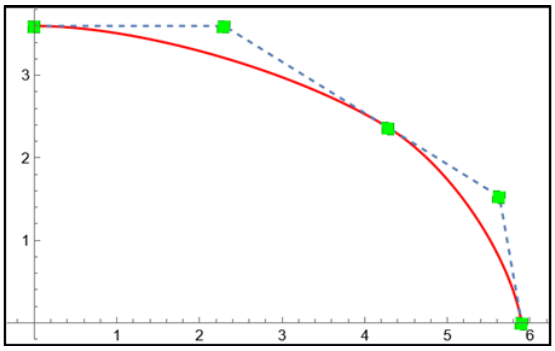

(c) Optimized bi-QT-Bézier ($r = 0.6765, \alpha = 2.299670, distance = 0.375021$)

Fig. 6. Comparison of biarc constructed with three different methods

Based on Table 4, the value of the shape parameter, m, varies between -1 and 1. When m is -1 or -0.5, the distance is 0.640200 and 0.507611, respectively. These values are bigger compared to the distance when $m = 0$. Hence, as the value of m is negative, the distance between the curve and the control polygon is getting farther. However, when the value of m is 0.5 or 1, the distance between the curve and the control polygon gets shorter. Therefore, a positive value of m will yield a shorter distance between the curve and the control polygon, thus, can help the biarc curve close to the control polygon.

Table 4
Distance between biarc and control polygon obtained from different values of m

Value of m	Distance
–1.0	0.640200
–0.5	0.507611
0.0	0.375021
0.5	0.242431
1.0	0.109841

In Figure 7, the biarc with $r = 0.6765,\ \bar{\alpha} = 2.299670$, are generated by setting the value of m as $m = -1$ (green), $m = -0.5$ (blue), $m = 0$ (red), $m = 0.5$ (black), and $m = 1$ (brown). From Figure 7, it is clear that the higher the value of m, the closer the curve is to the control polygon. Besides, the different values of m give different bi-QT-Bézier curve, which shows the flexibility of the proposed approach.

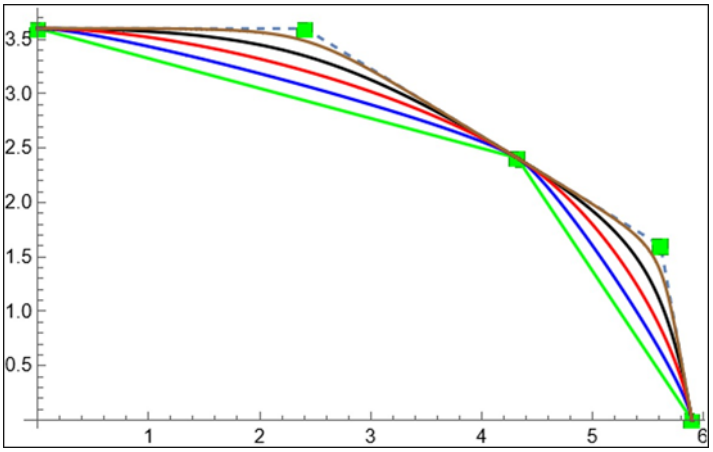

Fig. 7. Biarc constructed with different values of m; Green ($m = -1$); Blue ($m = -0.5$); Red ($m = 0$); Black ($m = 0.5$); Brown ($m = 1$)

Corollary 1: The curve formed by the bi-QT-Bézier is not a circular arc when the shape parameter m is non-zero. Even with m set to zero, the bi-QT-Bézier does not result in a biarc. It's crucial to note that, despite resembling the behavior of a quadratic Bézier when $m = 0$, the bi-QT-Bézier does not precisely create a circular arc.

3.2 Fitting a Circle

The proposed approach has been tested to fit a circle. Figures 8a and 8b show a circle composed of 12 data points of the proposed approach and the previous method by Park [1,2], respectively. The value of the ratio obtained for each biarc is recorded in Table 5. Note that the initial values used in computing the ratio for each biarc are; $d = 10, \rho = 0.25, r_u = 5, r_c = 1,$ and $r_l = 0.2$.

The ratio obtained for each biarc is used for both methods, optimized bi-QT-Bézier and optimal single biarc by Park [1,2]. Based on Table 5, the ratio, r for the biarcs, is between 0.77732 (Biarc 4) and 1.13125 (Biarc 5). In addition, the value of ratios can vary between the curve and the control polygon. Hence, it implies that the value of α and β is not necessarily equal to each other, as in Piegl and Tiller [3,4]. Notably, three biarcs have the same value of the ratio, $r = 1$. The result does not look abnormal as $r = 1$ is considered robust by Park [1,2] and Piegl and Tiller [3,4].

Table 5
The ratio obtained from 12 biarcs with its minimum distance

Biarc	Value of r	Minimum Distance
1	331/320	0.886870
2	1	0.797541
3	167/160	0.844142
4	192/247	0.845005
5	181/160	0.835871
6	523/480	0.861699
7	120/127	0.811085
8	1	0.841543
9	211/192	0.865280
10	333/320	0.810198
11	1	0.841543
12	960/973	0.814047

Correspondingly, the value of α is computed. For the proposed approach, the value of $\bar{\alpha}$ for each biarc is computed using PSO. Summarized in Table 6 are the results of $\bar{\alpha}$ computed for each biarc. The result also includes the shape parameter, m. It is worth mentioning that the value of m for all biarcs is set to be $m = 0.5$ so that the curve is closer to its control polygon but not too sharp to preserve the smoothness of the fitting curve. As shown in Figure 7, the curve with $m = 1$ has a sharper curve than $m = 0.5$. Therefore, intuitively, $m = 0.5$ will be used as the shape parameter. For the optimal single biarc approach, the value of α for each biarc is computed using Equation (3). The results of α for each biarc are also summarized in Table 7. Based on Tables 6 and 7, the value of $\bar{\alpha}$ is smaller compared to α as the solution space of PSO, $[Z_{min},\ Z_{max}]$ is set to be $[\alpha - \varepsilon,\ \alpha]$. Therefore, it is evident that $\bar{\alpha} \leq \alpha$ and based on Table 3, the smaller the α, the closer the distance between the curve and control polygon.

Table 6
The values of parameter m, ratio r and $\bar{\alpha}$ of every biarc generated by optimized bi-QT-Bézier

Biarc	p_0	p_4	θ_1 (Degree)	θ_2 (Degree)	m	Ratio, r	$\bar{\alpha}$
1	(98, 193)	(142, 181)	0	60	0.5	331/320	11.3928
2	(142, 181)	(171, 152)	330	30	0.5	1	10.4285
3	(171, 152)	(182, 110)	300	0	0.5	167/160	10.7727
4	(182, 110)	(172, 67)	270	330	0.5	192/247	12.6508
5	(172, 67)	(141, 37)	240	300	0.5	181/160	10.2667
6	(141, 37)	(98, 26)	210	270	0.5	523/480	10.8013
7	(98, 26)	(57.6, 36.5)	180	240	0.5	120/127	10.9128
8	(57.6, 36.5)	(27, 67.1)	150	210	0.5	1	11.0032
9	(27, 67.1)	(16, 110.3)	120	180	0.5	211/192	10.7980
10	(16, 110.3)	(27, 150.5)	90	150	0.5	333/320	10.3828
11	(27, 150.5)	(57.6, 181.1)	60	120	0.5	1	10.9770
12	(57.6, 181.1)	(98, 193)	30	90	0.5	960/973	10.5989

Table 7
The values of ratio r and $\bar{\alpha}$ of every biarc generated by optimal single biarc

Biarc	p_0	p_4	θ_1 (Degree)	θ_2 (Degree)	Ratio, r	$\bar{\alpha}$
1	(98, 193)	(142, 181)	0	60	331/320	11.4038
2	(142, 181)	(171, 152)	330	30	1	10.4308
3	(171, 152)	(182, 110)	300	0	167/160	10.8065
4	(182, 110)	(172, 67)	270	330	192/247	12.6587
5	(172, 67)	(141, 37)	240	300	181/160	10.3008
6	(141, 37)	(98, 26)	210	270	523/480	10.8069
7	(98, 26)	(57.6, 36.5)	180	240	120/127	10.9783
8	(57.6, 36.5)	(27, 67.1)	150	210	1	11.0062
9	(27, 67.1)	(16, 110.3)	120	180	211/192	10.8061
10	(16, 110.3)	(27, 150.5)	90	150	333/320	10.3895
11	(27, 150.5)	(57.6, 181.1)	60	120	1	10.0062
12	(57.6, 181.1)	(98, 193)	30	90	960/973	10.7872

Based on Table 8, the distances created by optimized bi-QT-Bézier are reduced by 35% compared to those created by optimal single biarc. From the results obtained in Tables 6 and 7, the biarcs are created and fit the circle. Figures 8a and 8b exhibit the biarc fitting of a circle using optimized bi-QT-Bézier and optimal single biarc.

Table 8
Comparison of the distance between the curve and polygon for each biarc created

Biarc	Distance by optimized bi-QT-Bézier	Distance by optimal single biarc
1	0.573318	0.886870
2	0.515566	0.797541
3	0.545497	0.844142
4	0.546217	0.845005
5	0.540417	0.835871
6	0.557038	0.861699
7	0.524321	0.811085
8	0.544011	0.841543
9	0.559352	0.865280
10	0.523749	0.810198
11	0.544095	0.841543
12	0.621280	0.814047

Based on Figure 8, both methods could fit the circle with 12 biarcs. Note that in this example, both methods have the same ratio, endpoints, and end tangents. The only difference between the optimized bi-QT-Bézier and the optimal single biarc is the value of the α and the inclusion of shape parameter m. Since both approaches have the same endpoints and end tangents, the number of biarc needed is also the same. Note that the circumference of the circle is 525.901. The total length for the curves formed using the optimized bi-QT-Bézier, and optimal single biarc are 524.9339 and 523.9518, respectively. Hence, the percentage error for the optimized bi-QT-Bézier is 0.18%, and for the optimal single biarc is 0.37%. Since the proposed approach has a lower percentage error than the optimal single biarc, it can be concluded that the optimized bi-QT-Bézier approximates better than the optimal single biarc.

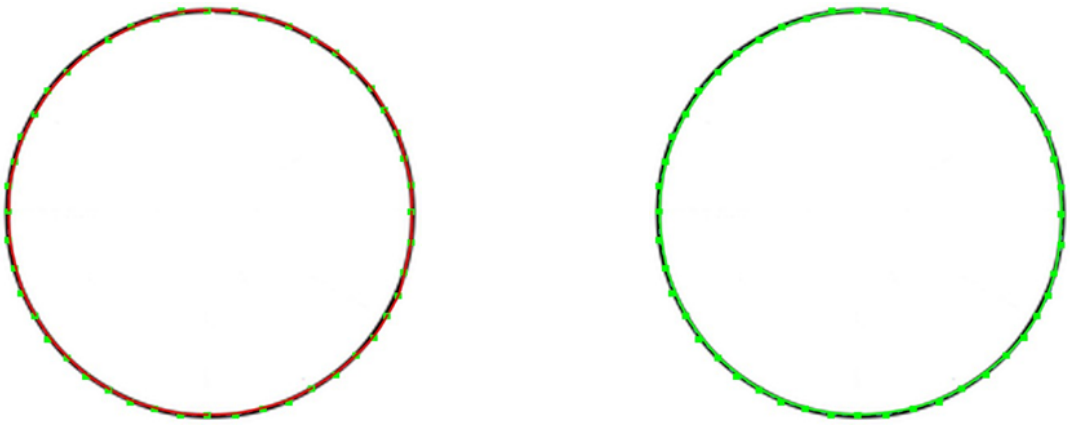

(a) Optimized bi-QT-Bézier (b) Optimal single biarc

Fig. 8. Fitting a circle that is composed of 12 points

Furthermore, the biarcs are analyzed by plotting the curvature plot. A curvature plot is a graphical representation that shows the curvature at a set of points along a curve. Curvature plots are used to analyze the smoothness of a curve. Figure 9 shows the curvature plot of the biarcs used to fit the circle. The orange curves are the curvature plot of biarcs generated by optimized bi-QT-Bézier, while the blue curves are biarcs generated by optimal single biarc. Notice the different shapes between both approaches. The optimized bi-QT-Bézier tends to have a mountain-like shape graphs, while the optimal single biarc have a U-shape graphs.

By comparing the shape of curvature plots by both approaches, it was evident that the curvature plot by optimal single biarc has a lesser variation value than the curvature plot by optimized bi-QT-Bézier. When a curvature plot has a minimum variation value, it has a fewer inflection points, hence, it can guarantee the smoothness of the curve. It implies that the biarcs generated by the optimal single biarc has a smoother curve compared to biarcs generated by optimized bi-QT-Bézier. This is because the optimized bi-QT-Bézier with shape parameter, $m = 0.5$, generates non-circular curves which affect the smoothness of the curve. Note that both approaches generate difference curvature plot for each curve. This is due to the different value of α obtained for every curves. Different α generates different curve with different curvature value.

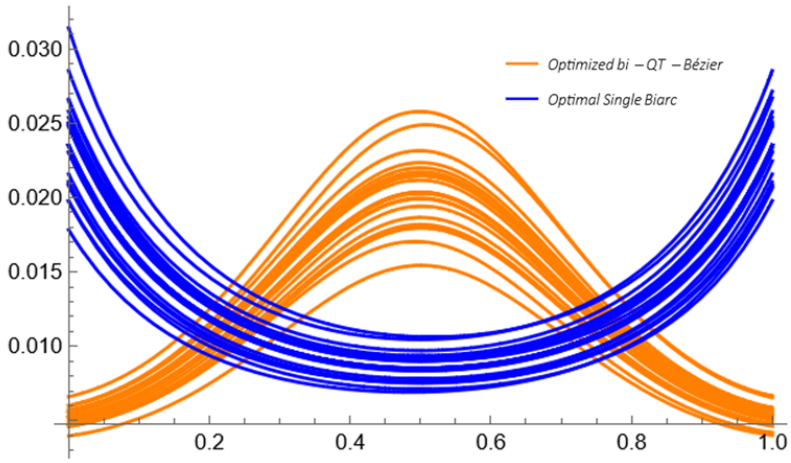

Fig. 9. Curvature plot of biarcs fitting a circle

Figure 10 shows the curvature plot of the curves generated by QT- Bézier with difference value of shape parameter, m. Based on Figure 10, the yellow curve has the smoothest curve compared to the others. This is because, when $m = 0$, the QT-Bézier imitates the ordinary quadratic Bézier which can generate a circular arc. Hence, the optimal single biarc is smoother than optimized bi-QT-Bézier as two circular arcs are joined to form a curve. It implies that when $m \neq 0$, the curves generate non-circular arcs and not become biarc but bi-QT-Bézier arc. Therefore, the curves have a slight variation based on the value of curvature. However, the proposed approach, the optimized bi-QT Bezier arc can provide more flexibility and the curve is approximate better than optimal single biarc as the curve is closer to the control polygon.

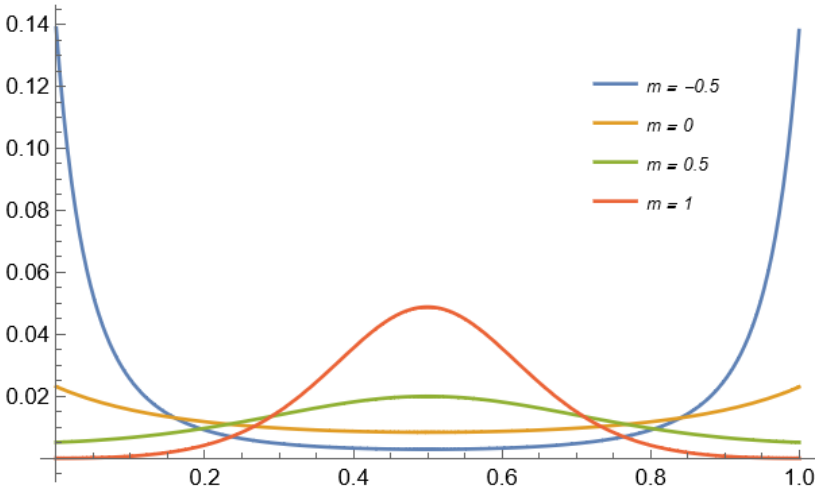

Fig. 10. Curvature plot of curves generated by QT-Bézier with different shape parameter, m.

3.3 Fitting a Complex Shape

The optimized bi-QT-Bézier and the optimal single biarc by Park [1,2] also have been implemented to fit a complex shape. The shape is composed of straight lines and curves. The example is aimed to analyze the relationship between the number of segments and the percentage error of the approximation. Figure 11 shows the optimized bi-QT-Bézier with 10 segments and the optimal single biarc with 10 and 12 segments, fitting a complex shape. The initial values used in computing the ratio for each biarc are $d = 10, \rho = 0.25, r_u = 5, r_c = 1$, and $r_l = 0.2$.

Based on Figure 11, it is clear that both approaches, optimized bi-QT-Bézier and optimal single biarc, could fit a straight line with only one segment. It is a special case where the collinear end tangents define the straight line, Piegl and Tiller [3]. However, when it comes to the curve, there are slight differences in the length of the biarc curve generated by optimized bi-QT-Bézier and optimal single biarc, even when the data points are the same. Note that the perimeter of the complex shape is 1318.27. The length of the biarc curve for each segment is recorded in Table 9.

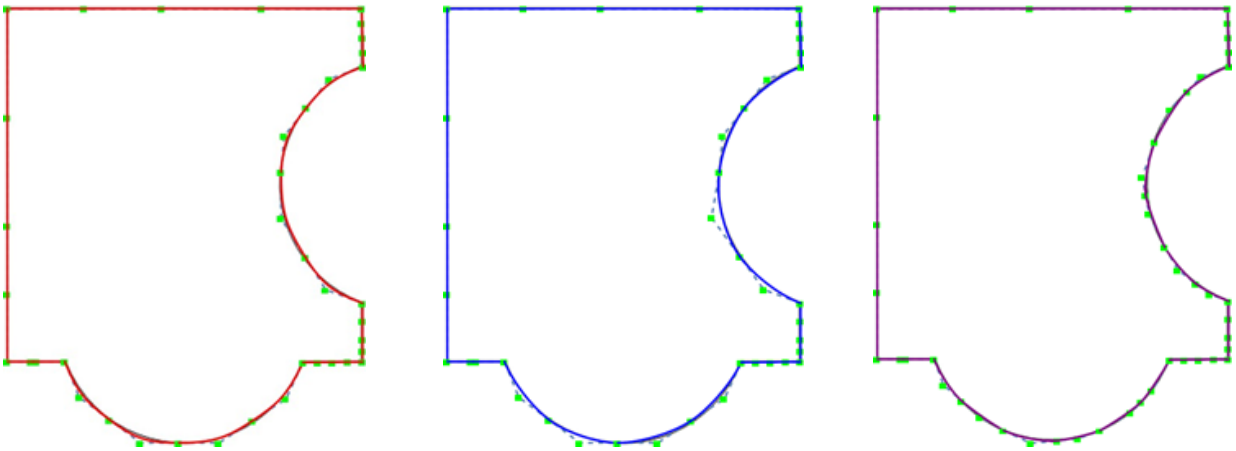

(a) Optimized bi-QT-Bézier (10 biarcs)

(b) Optimal single biarc (10 biarcs)

(c) Optimal single biarc (12 biarcs)

Fig. 11. Fitting a complex shape

Based on Table 9, the perimeter or the total length of the curves generated by optimized bi-QT-Bézier with ten segments is 1317.3709, which is a 0.07% of percentage error. On the other hand, the optimal single biarc with 10 segments has a total length of 1312.4490. Therefore, its percentage error is 0.44%. The optimized bi-QT-Bézier has a lower percentage error than the optimal single biarc with 10 segments. Hence, it indicates that the proposed approach approximates better when the same data points are used. However, the total length of the optimal single biarc with 12 segments is 1315.8097 with percentage error of 0.19%. In order to achieve a percentage error lower than 0.2%, the optimal single biarc needs to increase the number of segments. Therefore, it is clear that the approximation using the proposed approach, optimized bi-QT-Bézier requires a smaller number of curves than the optimal single biarc. The optimized bi-QT-Bézier reduces the number of curves by 16.67%.

Table 9
Length of the curve with different number of biarcs

Biarc	Optimized bi-QT-Bézier (10 biarcs)	Optimal single biarc (10 biarcs)	Optimal single biarc (12 biarcs)
1	49.8000	49.8000	49.8000
2	140.0400	138.6950	73.0120
3	120.3320	119.2360	94.0268
4	49.2146	49.2182	93.3148
5	300.000	300.0000	49.2182
6	299.2800	299.2800	300.0000
7	48.6000	48.6000	299.2800
8	126.7160	125.4430	48.6000
9	132.9860	131.7740	86.1197
10	50.4023	50.4028	85.1197
11			86.1494
12			50.4028
Total	1317.3709	1312.4490	1315.8097

Figure 12 shows the curvature plot of the biarcs used to fit the circular arcs as a part of the complex shape in Figure 11. The circular arcs that are located on the right side are labelled with solid curves, while dashed curves for the bottom part of the complex shape. Notice that the red curves (optimized bi-QT-Bézier with ten segments) have a mountain-like shape while the purple (optimal single biarc with ten segments) and black (optimal single biarc with 12 segments) curves have a U-shape graph. By comparing the purple and black curves, it is evident that black curves have higher curvature value at $t = 1$ than purple curves. This is due to the optimal single biarc with 12 biarcs have a smaller segment than optimal single biarc with ten biarcs. Notice that the dashed black curve overlaps with the solid black curve due to same curvature value generated for both right and bottom arcs.

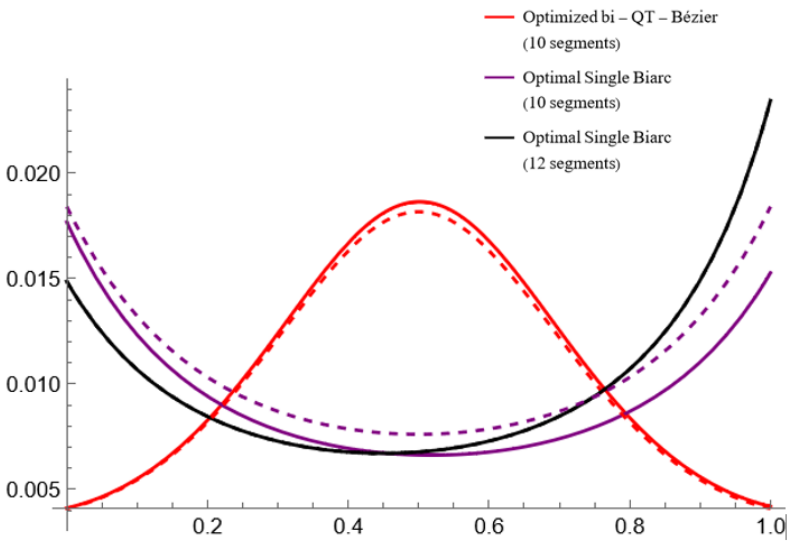

Fig. 11. Curvature plot of biarcs fitting the right (solid) and bottom (dashed) arcs of the complex shape

4. Conclusions

This paper proposes an optimized bi-QT-Bézier method to improve curve fitting. The proposed method integrates the optimal single biarc with Particle Swarm Optimization (PSO) and Quadratic Trigonometric (QT)-Bézier curve with a shape parameter. Other than that, this study obtained an optimized value of $\bar{\alpha}$ using the optimization method. The value of optimized $\bar{\alpha}$ yields a shorter distance between a biarc curve and its control polygon. This indicates that the biarc fitting approximation is better and more reliable. The QT-Bézier curve with a shape parameter helps to minimize the distance even more. The value of m can help pull the string of the curves to the control polygon using a higher value of m that is between 0 and 1. In addition, the QT-Bézier curve with a shape parameter also made the biarc more flexible.

This study analyzes the proposed approach to demonstrate its usefulness by applying it to fit a circle and complex shape. The results from the examples show that the optimized bi-QT-Bézier has a lower percentage error compared to the optimal single biarc. From the curvature analysis, it can be concluded that the curves generated by the optimal single biarc are smoother than the optimized bi-QT-Bézier. It is because the optimal single biarc generates two circular arcs that are joined to form a curve. However, the proposed approach, the optimized bi-QT Bezier arc can provide more flexibility and it approximate better than the optimal single biarc as the curve is closer to the control polygon. Moreover, the optimized bi-QT-Bézier could reduce the number of segments in curve fitting and become an excellent tool. Therefore, the proposed method can be very useful in the manufacturing industry, especially in Computer Numerical Control (CNC) milling machines. The method can minimize the error with a lower number of segments in 2D cutting process.

The limitation of this study is that the proposed approach only considers using QT-Bézier with a shape parameter. QT-Bézier with multi-shape parameters will provide better control of the curve's shape than QT-Bézier with single-shape parameters. Another optimization method, such as the Genetic Algorithm (GA), could also be applied to determine an optimal $\bar{\alpha}$.

Acknowledgement

This research is supported by Universiti Sains Malaysia under Short Term Grant (Khas) (304/PMATHS/6315587) and the School of Mathematical Sciences, Universiti Sains Malaysia. The authors are very grateful to the anonymous referees for their valuable suggestions.

References

[1] Park, Hyungjun. "Optimal single biarc fitting and its applications." Computer-Aided Design and Applications 1, no. 1-4 (2004): 187-195. https://doi.org/10.1080/16864360.2004.10738258
[2] Park, Hyungjun. "Error-bounded biarc approximation of planar curves." Computer-Aided Design 36, no. 12 (2004): 1241-1251. https://doi.org/10.1016/j.cad.2004.01.001
[3] Piegl, Les A., and Wayne Tiller. "Biarc approximation of NURBS curves." Computer-Aided Design 34, no. 11 (2002): 807-814. https://doi.org/10.1016/S0010-4485(01)00160-9
[4] Piegl, Les A., and Wayne Tiller. "Data approximation using biarcs." Engineering with computers 18, no. 1 (2002): 59-65. https://doi.org/10.1007/s003660200005
[5] Bolton, K. M. "Biarc curves." Computer-aided design 7, no. 2 (1975): 89-92. https://doi.org/10.1016/0010-4485(75)90086-X
[6] Meek, Dereck S., and Desmond J. Walton. "Approximation of discrete data by G1 arc splines." Computer-Aided Design 24, no. 6 (1992): 301-306. https://doi.org/10.1016/0010-4485(92)90047-E
[7] Schönherr, Jens. "Smooth biarc curves." Computer-Aided Design 25, no. 6 (1993): 365-370. https://doi.org/10.1016/0010-4485(93)90031-I
[8] Sabin, Malcolm Arthur. The use of piecewise forms for the numerical representation of shape. No. 60. MTA Számítástechnikai és Automatizálási Kutató Intézet, 1977.
[9] Ong, Chong Jin, Y. S. Wong, H. T. Loh, and X. G. Hong. "An optimization approach for biarc curve-fitting of B-spline curves." Computer-Aided Design 28, no. 12 (1996): 951-959. https://doi.org/10.1016/0010-4485(96)00028-0
[10] Gulsen, M., A. E. Smith, and D. M. Tate. "A genetic algorithm approach to curve fitting." International Journal of Production Research 33, no. 7 (1995): 1911-1923. https://doi.org/10.1080/00207549508904789
[11] Kumar, G. Saravana, Prem Kumar Kalra, and Sanjay G. Dhande. "Parameter optimization for B-spline curve fitting using genetic algorithms." In The 2003 Congress on Evolutionary Computation, 2003. CEC'03., vol. 3, pp. 1871-1878. IEEE, 2003. https://doi.org/10.1109/CEC.2003.1299902
[12] Ng, Win Son, Siew Chin Neoh, Kyaw Kyaw Htike, and Shir Li Wang. "Particle Swarm Feature selection for microarray Leukemia classification." Progress in Energy and Environment 2 (2017): 1-8.
[13] Gálvez, Akemi, and Andrés Iglesias. "Efficient particle swarm optimization approach for data fitting with free knot B-splines." Computer-Aided Design 43, no. 12 (2011): 1683-1692. https://doi.org/10.1016/j.cad.2011.07.010
[14] BiBi, Samia, Md Yushalify Misro, and Muhammad Abbas. "Shape optimization of GHT-Bézier developable surfaces using particle swarm optimization algorithm." Optimization and Engineering (2022): 1-21. https://doi.org/10.1007/s11081-022-09734-3
[15] Liu, Chengzhi, and Juncheng Li. "Study on the optimal shape parameter of parametric curves based on PSO algorithm." Journal of Interdisciplinary Mathematics 19, no. 2 (2016): 321-333. https://doi.org/10.1080/09720502.2015.1107317
[16] Eshan, Abdul Rauf, and Wah Yen Tey. "Investigation of Shape Parameter for Exponential Weight Function in Moving Least Squares Method." Progress in Energy and Environment 2 (2017): 17-24.
[17] Adnan, Sarah Batrisyia Zainal, Anis Aqilah Mohd Ariffin, and Md Yushalify Misro. "Curve fitting using quintic trigonometric Bézier curve." In *AIP Conference Proceedings*, vol. 2266, no. 1, p. 040009. AIP Publishing LLC, 2020. https://doi.org/10.1063/5.0018099
[18] Ismail, Nur Hidayah Mohammad, and Md Yushalify Misro. "Surface construction using continuous trigonometric Bézier curve." In *AIP Conference Proceedings*, vol. 2266, no. 1, p. 040012. AIP Publishing LLC, 2020. https://doi.org/10.1063/5.0018101
[19] Uzma, B., Muhammad Abbas, Mohd Nain Hj Awang, and Jamaludin Md Ali. "The quadratic trigonometric Bézier curve with single shape parameter." Journal of basic and applied scientific research 2, no. 3 (2012): 2541-2546.
[20] Han, Xuli. "Quadratic trigonometric polynomial curves with a shape parameter." Computer Aided Geometric Design 19, no. 7 (2002): 503-512. https://doi.org/10.1016/S0167-8396(02)00126-7
[21] Wu, Xiaoqin, Xuli Han, and Shanmin Luo. "Quadratic trigonometric spline curves with multiple shape parameters." In 2007 10th IEEE International Conference on Computer-Aided Design and Computer Graphics, pp. 413-416. IEEE, 2007. https://doi.org/10.1109/CADCG.2007.4407918
[22] Misro, Md Yushalify, Ahmad Ramli, Jamaludin Md Ali, and Nur Nadiah Abd Hamid. "Cubic trigonometric Bézier spiral curves." In 2017 14th International Conference on Computer Graphics, Imaging and Visualization, pp. 14-20. IEEE, 2017. https://doi.org/10.1109/CGiV.2017.27

[23] Misro, Md Yushalify, Ahmad Ramli, and Jamaludin Md Ali. "Extended analysis of dynamic parameters on cubic trigonometric Bézier transition curves." In *2019 23rd International Conference in Information Visualization–Part II*, pp. 141-146. IEEE, 2019. 10.1109/IV-2.2019.00036

[24] Xu, Wei Xiang, Liu Qiang Wang, and Xu Min Liu. "Quadratic TC-Bezier curves with shape parameter." In Advanced Materials Research, vol. 179, pp. 1187-1192. Trans Tech Publications Ltd, 2011. https://doi.org/10.4028/www.scientific.net/AMR.179-180.1187

[25] Engelbrecht, Andries P. Computational intelligence: an introduction. John Wiley & Sons, 2007. https://doi.org/10.1002/9780470512517